applied sciences

IMPACT FACTOR 2.7

CITESCORE 4.5

Review

Research Progress of Dynamic Measurement Technology of Atom Gravimeter

Chunfu Huang, An Li and Fangjun Qin

Special Issue

Recent Applications of Precise Measurement and Metrology with Atomic, Optical and Molecular Systems

Edited by
Dr. Marco Tarallo

MDPI

https://doi.org/10.3390/app13158774

applied sciences

MDPI

Review

Research Progress of Dynamic Measurement Technology of Atom Gravimeter

Chunfu Huang, An Li and Fangjun Qin *

School of Electrical Engineering, Naval University of Engineering, Wuhan 430033, China
* Correspondence: haig2022@126.com

Abstract: After more than 30 years of development, the measurement performance of atom gravimeters in the laboratory has reached a high level. More and more compact, small, portable instruments begin to appear, and field measurements have been conducted gradually. At present, the field measurements of atom gravimeters are mostly static or "stop-and-go" quasi-dynamic experiments, and the research on dynamic measurement is still in its infancy. High-precision absolute gravity dynamic surveying in the field has shown attractive prospects in many aspects, and many researchers have carried out research on it. This paper first reviews the main research work of the atom gravimeter, especially its dynamic measurement technology. Then it introduces the reported principle, scheme, and equipment of atom gravimeter dynamic measurement. The generation mechanism and suppression methods of the main error sources of dynamic measurement, such as vibration noise, accelerometer drift, and carrier dynamic effect, are analyzed. Finally, the application prospects of atom gravimeter dynamic measurement technology in gravity field mapping, navigation, and underwater target detection are discussed.

Keywords: atom gravimeter; dynamic measurement; accelerometer; vibration noise; Eötvös correction; tilt correction

Citation: Huang, C.; Li, A.; Qin, F. Research Progress of Dynamic Measurement Technology of Atom Gravimeter. *Appl. Sci.* **2023**, *13*, 8774. https://doi.org/10.3390/app13158774

Academic Editor: Marco Tarallo

Received: 21 June 2023
Revised: 26 July 2023
Accepted: 27 July 2023
Published: 29 July 2023

1. Introduction

With the advent of laser cooling technology in the 1980s, scientists were able to capture and manipulate originally "active" atoms. In 1991, the Steven Chu research team at Stanford University realized an atom interferometer for the first time by using the method of stimulated Raman transition [1]. For more than 30 years, atom interference technologies have developed rapidly. At present, more than 50 research groups in the world have devoted themselves to the research of atom interferometers. It is widely used in the fields of navigation [2,3], metrology [4,5], gravitational wave detection [6], and general relativity verification [7,8].

Among them is the most in-depth and representative research on the use of atom interference technology for gravity measurement, i.e., the atom gravimeter. The atom gravimeter measures the absolute gravity value. Compared with the relative gravimeter with a straight-pull or zero-length spring, there is no mechanical wear, no drift, and no need for periodic correction. Compared with the optical interference absolute gravimeter, its wavelength is much shorter, so it has higher potential sensitivity and accuracy according to the relationship between the wavelength of matter waves and particle momentum [9]. Atomic gravimeters are expected to surpass relative gravimeters and optical interference gravimeters to become the next generation of high-precision absolute gravity sensors [10–12].

In the early days of the development of atom gravimeters, various research teams devoted themselves to improving the sensitivity, accuracy, and stability of the system in the laboratory environment. For example, when Steven Chu's team demonstrated the atom interferometer for the first time, it was used to measure gravity. The Raman light interval

time T was 10 ms, and the measurement resolution was 3 mGal (1000 s) [1]. In 2001, the team developed the second-generation instrument, and its performance greatly improved. Under the condition of T being 160 ms, the fountain-type atom gravimeter was realized by using a cesium atom cloud with a sensitivity of 20 μGal/Hz$^{1/2}$ and a resolution of 0.1 μGal (48 h). The system error and noise source were analyzed in detail, and the comprehensive uncertainty was 3.4 μGal [13]. In 2008, cesium atoms were continued to be used under the condition of a longer Raman interval time (400 ms), and the measurement sensitivity was 8 μGal/Hz$^{1/2}$ [14]. Huazhong University of Science and Technology has been conducting research on atom gravimeters in cave laboratories since 2006, with the goal of achieving a sensitivity of 1 μGal/Hz$^{1/2}$ [15]. In 2013, the team used a two-dimensional magneto-optical trap to increase the number of atoms, improve the signal-to-noise ratio, use a better optical phase-locked loop to reduce the phase noise of Raman light, and combine it with an active vibration isolation system to obtain a sensitivity of 4.2 μGal/Hz$^{1/2}$ [16]. In addition, there are many research teams dedicated to the study of atom gravimeters. Table 1 lists some of the reported static measurement results of high-precision atom gravimeters.

Table 1. Reported static measurement results of high-precision atom gravimeters.

Research Teams	Raman Light Interval Time (ms)	Sensitivity (μGal/Hz$^{1/2}$)	Uncertainty (μGal)	Resolution (Integration Time) (μGal)
French Aerospace Lab (ONERA) [17]	48	42	25	— [1]
LNE-SYRTE, Observatoire de Paris [18–20]	80	5.7	4.3	0.2 (3 h)
Humboldt Universitat zu Berlin [21]	260	9.6	3.2	0.05 (105 s)
the University of California, Berkeley [22]	130	37	15	2 (0.5 h)
Wuhan Institute of Physics and Mathematics [23,24]	200	28	9	1 (4000 s)
Zhejiang University of Technology [25]	70	90	19	—
National institute of metrology, China [26]	70	44	5.2	0.2 (30,000 s)

[1] "—" means not evaluated.

In recent years, research teams have paid more attention to the integration and miniaturization of devices. For example, in 2010, Q. Bodart et al. proposed a miniaturization scheme using a pyramid mirror to achieve atomic capture, state selection, interference, detection, and other functions with a single laser beam. This scheme greatly reduced the complexity and volume of the system. The sensitivity of the system was 170 μGal/Hz$^{1/2}$ [27]. Inspired by this, some teams have adopted a similar structure to design atom gravimeters [22,28]. In 2014, B. Wu et al. improved the magnetic shielding coil of the atom gravimeter to replace the traditional metal shield and adopted a relatively small portable vibration isolation platform, which provided a new realization method for field measurement. The sensitivity was 100μGal/Hz$^{1/2}$, and the integral resolution of 1000 s was 5.7 μGal [29]. 2016. Q. Y. Wang et al. improved the laser system with a modular design and applied it to an atom gravimeter for gravity measurement. The integral resolution of 200 s was 10 μGal [30]. More and more portable atom gravimeters are gradually coming out of the laboratory to carry out measurements in the field. For example, in 2019, X. J. Wu et al. used a pickup truck to carry an atom gravimeter to measure the absolute gravity values at six different elevations in the Berkeley Mountains and obtain the relationship between gravity anomalies and height. The sensitivity was 500 μGal/Hz$^{1/2}$, and the uncertainty was 40 μGal [22]. In 2020, B. Wu et al. integrated a set of vehicle-mounted absolute gravity measurement systems using a miniaturized atom gravimeter developed by themselves

and carried out surveying and mapping work in the field. They conducted repeated line measurements on flat roads and obtained an internal coincidence accuracy of 30 μGal. They measured gravity values at different altitudes on mountain roads with large inclination angles and obtained vertical gravity gradient values [31]. In 2021, J. Y. Zhang et al. used a vehicle-mounted mobile gravimeter to measure the gravity values of 29 points on the mountain. Based on this, the density distribution of the mountain was inverted, which was consistent with the actual geological exploration results [32].

Although the atom gravimeter has achieved high performance in the field under static or "stop-and-go" quasi-dynamic conditions, there are few reports on dynamic measurement, i.e., gravity measurement during carrier motion. The research team first carried out dynamic experiments under very low-speed conditions. In 2009, a Stanford University team performed gravity gradient measurements on a low-speed truck at 1 cm/s [33]. In 2022, Zhejiang University of Technology (ZJUT) carried out a low-speed traction test in the laboratory. At the maximum traction speed of 5.5 cm/s and the maximum vibration amplitude of 0.1 m/s^2, the measurement results were in good agreement with the values under static conditions, with an accuracy of (-1.22 ± 2.42) mGal [34]. ONERA is a pioneer in the study of the dynamic measurement of atom gravimeters. In 2013, they first carried out gravity measurements on a moving elevator, and the results were consistent with the static measurements, which verified the feasibility of the atom gravimeter's dynamic measurement [17]. Since then, they have carried out dynamic measurement experiments under ship-borne and air-borne conditions, respectively, and obtained good measurement results. In the ship-borne test, compared with the gravity-calibrated route, the accuracies of forward and backward were respectively (-0.2 ± 0.5) mGal and (-0.6 ± 0.3) mGal [35]. In the air-borne test, compared with the upward continuation of ground gravity data, the accuracies of repeated and cross lines were (-1.9 ± 3.3) mGal and (-0.7 ± 6.2) mGal, respectively. The accuracy was (-0.8 ± 3.3) mGal when the laser misalignment area was removed from the cross-measurement line [36]. In the later air-borne test, the measurement accuracy was further improved to 0.6~1.3 mGal [37]. ZJUT team also carried out dynamic tests. In addition to low-speed traction in the laboratory, they also carried out a sea navigation test. Compared with the XGM2019 earth gravity model, the measurement accuracy of (2.6 ± 13.6) mGal, (3.4 ± 15.3) mGal, and (-0.3 ± 8.1) mGal were obtained at average speeds of 22.6 km/h, 14.3 km/h and 2.1 km/h, respectively [38].

The author's team has gradually carried out research on the atom gravimeter, especially its dynamic measurement technology. We developed a dynamic measurement test system for an atom gravimeter, which has a measurement sensitivity of 447 μGal/Hz$^{1/2}$ and a long-term stability of 2.7 μGal under static conditions in the laboratory. We first used the self-developed test system to carry out experiments on the laboratory swing table, simulating the pitch and roll of the ship during navigation, and verified the feasibility of applying the equipment and method to the dynamic conditions of navigation. Then, we carried out an experiment in a certain lake area, as shown in Figure 1. Under the condition of the highest speed of 8.6 km/h, the external coincidence accuracies of the four voyages were 2.331 mGal, 1.837 mGal, 3.988 mGal, and 2.589 mGal, respectively. In addition, to meet the real-time requirements of dynamic measurement, the Kalman filter method was used for data processing, and the gravity value was obtained in real time. The measurement accuracy was (2.03 ± 7.12) mGal [39,40]. Compared with the current gravimeters, especially ONERA's [35], our system still has some room for optimization. In the follow-up, we will continue to improve the system structure, optimize the measurement algorithm, and carry out sea navigation measurement experiments with severe sea conditions to further improve the accuracy and verify the stability and environmental adaptability of the system.

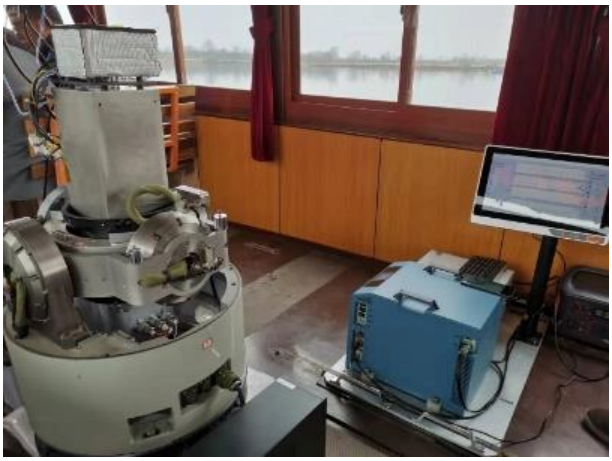

Figure 1. Atom gravimeter for dynamic measurement from authors' team.

This paper focuses on the research progress of the atom gravimeter in dynamic measurement. Firstly, the principle, scheme, and device of atom gravimeter dynamic measurement are described. Secondly, the main error sources and suppression methods of atom gravimeter dynamic measurement are analyzed. Finally, the possible application direction of atom gravimeter dynamic measurement technology is discussed.

2. Dynamic Measuring Principle and Device of Atom Gravimeter

2.1. Basic Principles of Atom Gravimeter

To measure the gravitational acceleration, the atoms are cooled and trapped by a three-dimensional magneto-optical trap in a vacuum environment. The atoms are further cooled to the order of μK by polarization gradient cooling, and then the light field is turned off so that the atoms fall freely under the action of gravity. As shown in Figure 2, the π/2-π-π/2 laser pulses formed by the reflecting mirror are used to split, reflect, and combine the falling cold atoms, and the M-Z interference is realized. The acceleration information of the atoms relative to the mirror is transferred to the interference fringes. The phase difference of the atom interference between the two paths is $\Delta\phi = k_{\text{eff}} \cdot gT^2$, where $k_{\text{eff}} \simeq 4\pi/\lambda$ is the effective wave vector of two backpropagating Raman beams, λ is the wavelength of the laser, and T is the time interval between the two Raman beams.

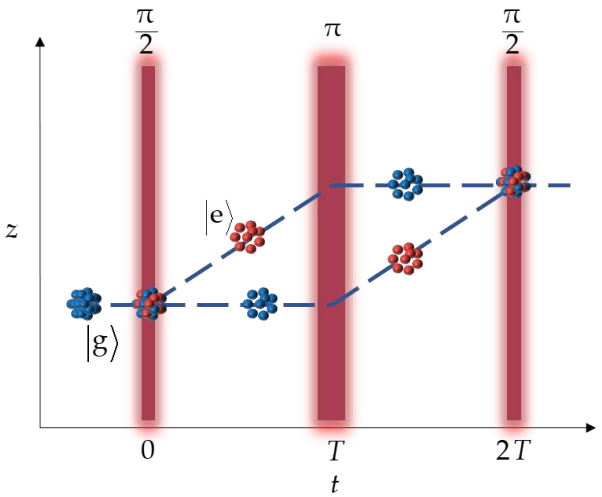

Figure 2. The actions of three Raman beams on atom cloud.

In order to compensate for the Doppler shift during the free-fall of the atoms, a linear chirp sweep must be performed on the frequency difference between the two Raman beams. At this time, the interference phase difference can be expressed as

$$\Delta\phi = (k_{\text{eff}} \cdot g - 2\pi\alpha)T^2. \tag{1}$$

When the chirp rate $\alpha = k_{\text{eff}} \cdot g/2\pi$, the Raman optical phase shift is exactly the same as the gravitational phase shift.

In the process of interference, the internal state of the atom changes. At the initial moment, the atoms are in the $|g\rangle$ state, and after the action of the first $\pi/2$ Raman light, some of the atoms transition to the $|e\rangle$ state. The atoms in $|g\rangle$ transition to $|e\rangle$ and the atoms in $|e\rangle$ transition to $|g\rangle$ when the second π Raman beam actions. After the third Raman beam, the atomic wave packets combine and interfere. The population of atoms in $|e\rangle$ state after interference is measured by fluorescence signal, and its relationship with gravity phase shift is

$$P = P_0 - \frac{C}{2}\cos\Delta\phi, \tag{2}$$

where P_0 is fringe offset and C is contrast. Under static conditions, because the gravity value is basically unchanged, a number of interference fringes can be fitted by changing the chirp rate α and Raman light interval time T, and the corresponding gravity value at the center of the fringe is the local gravity value [1,13,40,41], as shown in Figure 3.

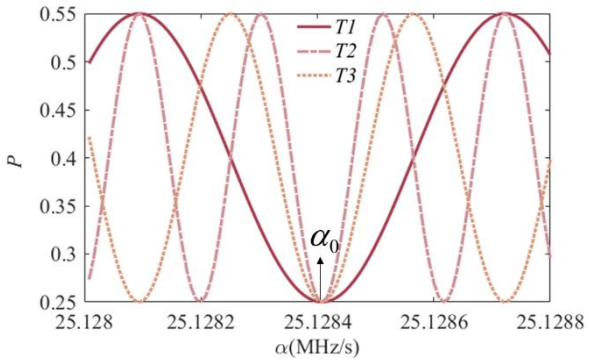

Figure 3. Interference fringe and fringe center.

2.2. Dynamic Measurement Principle of Atom Gravimeter

In a dynamic environment, the gravity value varies with the movement of the carrier position. If the gravity value is calculated by changing T to obtain the center of the fringe as in the static state, the data rate will inevitably be greatly reduced. For example, ZJUT takes the results of fringe fitting as a comparison item in the dynamic experiment, and the data rate is only 1/59 Hz [38]. In addition, the atom gravimeter measures the acceleration of atoms relative to the mirror; the carrier movement causes the mirror itself to generate vibration acceleration a_{vib}. And a_{vib} is often greater than the dynamic range corresponding to a fringe period, which leads to the gravity information being submerged in vibration noise, and it is almost impossible to obtain the gravity value through fringe fitting. Most research teams use an accelerometer (or seismometer) and an atom gravimeter for combined measurement and adopt different schemes to take advantage of the two to solve the above problems. At present, there are the following data processing schemes.

2.2.1. Coarse-Fine Combination

The scheme of ONERA is the Coarse-fine combination, and the specific process is as follows. Within a measurement period, the atom gravimeter obtains the population $P(t)$, and the possible gravity value is obtained by reverse solving Equation (2):

$$g_{\mathrm{at}}(t,s,n) = \frac{s \times \arccos\left[2\frac{P_0-P(t)}{C}\right] + 2\pi \times n}{k_{\mathrm{eff}}T^2} + \frac{2\pi\alpha}{k_{\mathrm{eff}}}. \tag{3}$$

However, for a measured population, there are multiple possible gravity values corresponding to it, where $s = \pm 1$, and n is an integer, which represents the multi-valued property of the measurement. In the case of little fluctuation in environmental factors such as temperature, the changes in parameters P_0 and C are relatively small [42,43]. Generally, these parameters are either obtained by fringe fitting in static measurement, set as fixed values in dynamic measurement, or estimated by the average value and standard deviation of the output signal of the atom gravimeter [6]. The chirp rate α is determined by

$$\alpha = \pm 1\left(k_{\mathrm{eff}} \times g_{\mathrm{prev}} + \frac{\mathrm{rnd}(2\pi)}{T^2}\right), \tag{4}$$

where g_{prev} is the result of the previous measurement period, and the sign of α is changed alternately with the measurement period to eliminate some systematic errors [35,36].

While the sampling rate of the accelerometer is usually higher, the gravity sequence $g_{\mathrm{acc}}(t\prime)$ can be obtained with the same period, which is convolved with the sensitivity function of the atom gravimeter $h(t\prime)$ to obtain a rough estimate of gravity within the measurement period:

$$g_{\mathrm{acc}}(t) = \int_{-T}^{T} g_{\mathrm{acc}}(t_\pi + t\prime)h(t\prime)\mathrm{d}t\prime, \tag{5}$$

$$h(t\prime) = \begin{cases} \frac{T+t\prime}{T^2}, -T \le t\prime \le 0 \\ \frac{T-t\prime}{T^2}, 0 \le t\prime \le T \end{cases}, \tag{6}$$

where t_π represents the time corresponding to the π pulse. Find the closest $g_{\mathrm{at}}(t,s,n)$ to the value, and n and s in Equation (3) can be determined. Then the multi-value of the atom gravimeter output can be eliminated and a definite value $g_{\mathrm{at}}(t)$ can be obtained. The data processing flow of the coarse–fine combination is shown in Figure 4.

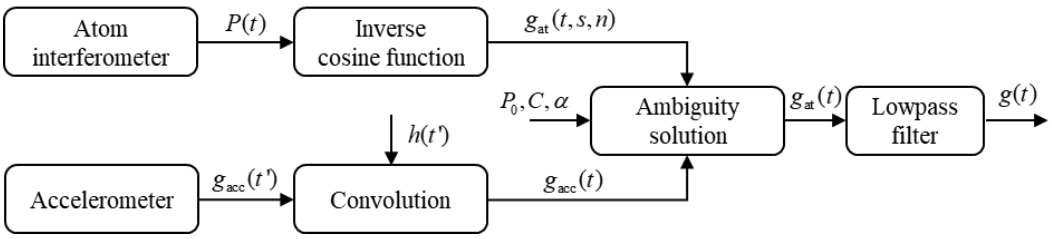

Figure 4. Flow chart of coarse–fine combination data processing.

The dynamic range corresponding to one fringe period of the atom gravimeter can be calculated by Equation (2) as $2\pi/k_{\mathrm{eff}}T^2$, and for a gravimeter T = 15 ms, it is only about 170 mGal. However, the general accelerometer is above 1 g, and some can even reach hundreds of g. Therefore, when the accuracy of the accelerometer is better than $2\pi/k_{\mathrm{eff}}T^2$, the coarse-fine combination has a good effect. While solving the multi-valued problem, this scheme can improve the dynamic range of the atom gravimeter to be comparable to that of the accelerometer [11,22,44–48].

In this scheme, the vibration noise is mainly filtered by offline low-pass filtering of the output data, so it is more suitable for scenarios such as gravity map mapping and resource exploration that do not require high real-time performance.

2.2.2. Kalman Filter

When the measured gravity data is used for navigation, detection, and other scenarios, real-time performance is more emphasized. Therefore, teams such as French iXBlue and ZJUT have adopted another scheme, i.e., using data fusion algorithms such as the Kalman filter to estimate the gravity value in real-time. The effect of vibration acceleration a_{vib} on the reflecting mirror of an atom gravimeter is equivalent to the introduction of an additional phase shift in gravity phase shift

$$\Delta\phi = (k_{\text{eff}} \cdot g - 2\pi\alpha)T^2 + \phi_{\text{vib}}. \tag{7}$$

The accelerometer can be firmly connected to the mirror to measure the vibration, and the vibration can be converted into the corresponding phase shift to correct the gravity phase shift:

$$\phi_{\text{vib}} = k_{\text{eff}} \int_{-T}^{T} a_{\text{acc}}(t_\pi + t\prime)h(t\prime)\mathrm{d}t\prime. \tag{8}$$

The fringe parameters P_0, C and the gravity value g are taken as state vector, i.e., $\boldsymbol{X} = \begin{bmatrix} P_0 & C & g \end{bmatrix}^{\mathrm{T}}$. The evolution of the state vector over time is

$$\boldsymbol{X}_k = \boldsymbol{F} \cdot \boldsymbol{X}_{k-1} + \boldsymbol{w}, \tag{9}$$

where, $\boldsymbol{X}_k$ and $\boldsymbol{X}_{k-1}$ are the states at k and $k-1$ moment respectively, and $\boldsymbol{F}$ is the state evolution matrix:

$$\boldsymbol{F} = \begin{pmatrix} 1 & 0 & 0 \\ 0 & 1 & 0 \\ 0 & 0 & 1 \end{pmatrix}. \tag{10}$$

$\boldsymbol{w}$ is the process noise of the state vector $\boldsymbol{X}$, and its covariance matrix can be represented by a diagonal matrix:

$$\boldsymbol{Q} = \begin{pmatrix} \sigma_{P_0}^2 & 0 & 0 \\ 0 & \sigma_C^2 & 0 \\ 0 & 0 & \sigma_g^2 \end{pmatrix}, \tag{11}$$

where σ_{P_0}, σ_C and σ_g are a priori statistics of the standard deviation of P_0, C and g, respectively.

The population of the atom gravimeter $P(k)$ is observed, and the observation noise v can be expressed by the diagonal matrix $\boldsymbol{R}$. The dimension of $\boldsymbol{R}$ is 1, and the value is σ_P^2, i.e., the prior variance of the population P. The observation matrix $\boldsymbol{H}$ is the Jacobian matrix of the state vector with respect to the observation equation:

$$\boldsymbol{H} = \begin{pmatrix} 1 \\ -\frac{1}{2}\cos\left[(k_{\text{eff}} \cdot g - 2\pi\alpha)T^2 + \phi_{\text{vib}}\right] \\ \frac{C \cdot k_{\text{eff}} \cdot T^2}{2} \sin\left[(k_{\text{eff}} \cdot g - 2\pi\alpha)T^2 + \phi_{\text{vib}}\right] \end{pmatrix}^{\mathrm{T}}. \tag{12}$$

Under the framework of extended Kalman filter, the gravity value can be estimated in real-time by iterative recursion [38,42,49].

2.3. Dynamic Measurement Device of Atom Gravimeter

Although the combination algorithms of different research teams vary, the dynamic measurement device of the atom gravimeter is roughly the same. The dynamic measurement device mainly includes three parts: an atom gravimeter, an accelerometer, and a dual-axis stabilized platform. The atom gravimeter mainly includes a vacuum system, an optical system, and a control system. The vacuum system is the site for atomic trapping, falling, and detection, and the vacuum environment is helpful to reduce the influence of air resistance. The optical system provides lasers with different polarizations, powers, and frequencies needed in the working process of the atom gravimeter. The control system realizes the functions of sequential control, signal acquisition, and algorithm operation. The

accelerometer is fixed on the mirror to measure the vibrational acceleration or gravitational acceleration near the vacuum sensor. The vacuum sensor and the accelerometer are placed on the dual-axis stabilized platform so that the direction of the Raman light wave vector coincides with the gravity direction during the motion. This reduces the influence of the inclination angle [50] and ensures that the atom gravimeter and accelerometer measure the acceleration in the vertical direction. The inertial measurement unit in the stabilized platform can not only provide the attitude reference for the platform but also output navigation information such as the velocity and position of the carrier, which is used for subsequent Eötvös correction and accuracy assessment for the gravity output from the test system. In order to improve the accuracy of navigation and attitude, a navigation solution scheme combining inertial navigation and the global navigation satellite system is usually adopted. Figure 5 shows the schematic diagram of the dynamic measurement device of the atom gravimeter of the author's team [40].

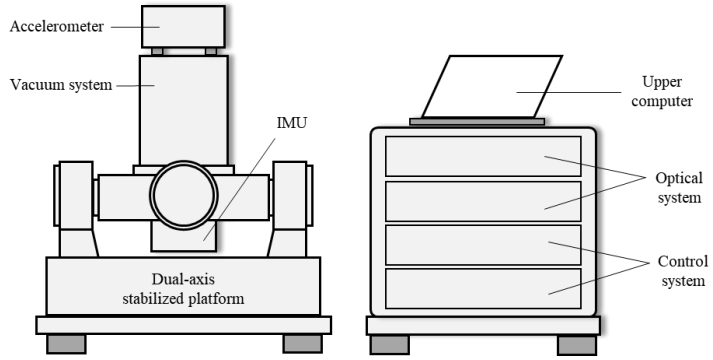

Figure 5. Dynamic measurement device of atom gravimeter of the authors' team.

3. Main Error Sources and Suppression Methods of Dynamic Measurement

The atom gravimeter has excellent performance in laboratories where environmental factors are well controlled, and its sensitivity and accuracy can exceed those of a classical gravimeter, but its volume is usually large. The atom gravimeter hat can be used for field measurement and requires high stability and reliability, as well as small size, easy movement, low power consumption, and so on. Under dynamic conditions, the atom gravimeter not only needs to have the above characteristics but also needs to overcome the additional vibration noise introduced in the dynamic environment and the influence of system effects. The main error sources and suppression methods of atom gravimeter dynamic measurement are listed below.

3.1. Vibration Noise

As shown in Figure 6, because two beams of Raman light propagating in the opposite direction are needed to increase the effective wave vector and improve the sensitivity, one beam of light needs to be reflected by the mirror. However, the ground vibration will lead to the displacement of the position of the mirror δz and the phase shift of the reflected Raman light, which is coupled to the gravity phase and results in an inaccurate gravity measurement. Because of the high sensitivity of the atom gravimeter, even low-level vibration may exceed its measuring range of gravity, resulting in blurred interference fringes. Under dynamic conditions, the level of vibration noise is higher, which is the main source of error and limits the accuracy of atom gravimeters.

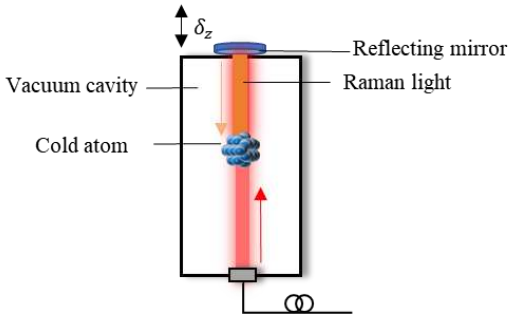

Figure 6. Raman reflecting mirror generates vibration noise with ground vibration.

There are mainly three methods for suppressing vibration noise: passive vibration isolation based on super springs [51], active vibration isolation with feedback control [52–54], and using a motion sensor such as a seismometer or accelerometer to measure vibration noise and compensate [46,48]. In practical application, in the case of obvious external vibration and large interference, the vibration compensation method has a better effect than the active and passive vibration isolation methods. Moreover, the vibration isolation device is often complex and not easy to carry, and it is not suitable for the field dynamic measurement scene. Therefore, the vibration compensation method is generally used to suppress the vibration noise in the dynamic measurement scene. This method was first proposed in 2009 by S. Merlet et al., who compared it with fringe fitting and nonlinear phase-locking and achieved a sensitivity of 55 $\mu Gal/Hz^{1/2}$ in the absence of vibration isolation in the center of Paris [48]. In 2019, Hanover University compared the performance of various types of accelerometers and seismometers using post-correction, pointing out that seismometers that are more sensitive to low-frequency motion are suitable for low inertial noise environments, while accelerometers with high dynamic range perform better in high inertial motion environments [55]. The method of using accelerometers or other vibration sensors to suppress the influence of vibration noise under dynamic measurement conditions has been provided in the previous Principle and Device section and will not be repeated.

3.2. Error from Accelerometer

Whether it is the compensation of vibration noise or the rough estimate of gravity value, the accelerometer is required to have high precision, so the error of the accelerometer itself cannot be ignored. However, due to the influence of environmental factors such as temperature or the structure of the device itself, the accelerometer drifts. For example, the commonly used Nanometrics Titan accelerometer has a temperature drift coefficient of 320 mGal/°C [56], which affects the measurement accuracy of the final gravity value. The following methods can be used to inhibit accelerometer drift: The first is to add a temperature control system; for example, the atom gravimeter laboratory transformed from a container in ZJUT installs an air conditioning temperature control device to maintain the ambient temperature and humidity and make the instrument work normally [38]. The second is to model and compensate the temperature drift of the accelerometer, collect the drift data at different temperatures, establish the drift model, and compensate through the algorithm, which can effectively suppress the temperature drift and obtain high-precision acceleration signals. Figure 7 shows the scene of our accelerometer temperature experiment. The third is to compare the exact gravity value obtained by the atom gravimeter with the one obtained by the accelerometer to get the drift value and deduct it. The three methods involve the whole process of measurement, do not conflict with each other, and can be used all or only a few of them.

Figure 7. Scene of accelerometer temperature experiment.

In addition, due to the different installation positions of the accelerometer and the Raman reflecting mirror, there is a mechanical transfer function. If the output of the accelerometer is directly used for vibration compensation, it cannot reflect the real vibration noise. This is an important factor affecting the vibration compensation, so the transfer function needs to be calibrated before measurement. Many scholars have carried out relevant studies on the transfer function. For example, based on the simplified transfer function model including delay and gain coefficients, J. M. Yao et al. analyzed the interference fringes of the atom gravimeter and the output signal of the accelerometer and searched for the optimal values of the two coefficients in the current environment, which can more accurately speculate the real vibration of the mirror in the current environment [57]. W. B. Gong et al. used the improved chaotic sparrow search algorithm to optimize the above two coefficients, which can achieve a good compensation effect in a short period of time. After compensation, the uncertainty of fringe fitting was attenuated by 70.21%, and the search time was shortened nearly six times, effectively improving the accuracy and stability of the atomic gravimeter [58].

3.3. Dynamic Effect of the Carrier

3.3.1. Eötvös Effect

Gravity is the resultant force of universal gravitation and the inertial force corresponding to the centripetal force of the earth's rotation. When the gravity measurement is carried out on the motion carrier, the instrument is moving relative to the earth, which is affected by the Coriolis acceleration. The superposition of the carrier velocity and the earth rotation velocity vector changes the inertia force, which leads to the deviation between the observed gravity and reality, which is called the Eötvös effect. The Eötvös effect correction is made for the gravity measurement, and its value is

$$\delta a_c = 2\omega_e v_E \cdot \cos\varphi + \frac{v_E^2}{R_N + h} + \frac{v_N^2}{R_M + h}, \quad (13)$$

where ω_e is the angular velocity of the earth's rotation, R_N and R_M are the radius of curvature in the meridian and prime vertical of the earth, respectively, v_E and v_N are the eastward and northward velocities of the carrier, φ is latitude, and h is height.

Although the influence of Eötvös effect on gravity measurement can reach the order of mGal, it can be greatly reduced by the high-precision velocity and position information provided by the navigation system of the carrier.

3.3.2. Horizontal Acceleration

The stabilized platform provides a horizontal reference for the atom gravimeter to ensure that it measures the acceleration in the vertical direction. However, due to the

influence of the dynamic environment and the limitations of the technical performance of the platform itself, the platform cannot be absolutely horizontal. There is an inclination angle, and gravity measurements will inevitably be disturbed by the horizontal acceleration of the carrier. Therefore, it is necessary to establish a model and correct it, which is called horizontal acceleration correction or tilt correction.

The researchers have proposed a variety of correction models, which can be divided into two categories. One is to directly use accelerometer measurements and navigation information to calculate the correction:

$$\delta a_{\mathrm{H}} = (f_x^2 + f_y^2 - a_{\mathrm{E}}^2 - a_{\mathrm{N}}^2)/2g_{\mathrm{m}}, \tag{14}$$

where, f_x and f_y are the lateral and longitudinal horizontal accelerations sensitive to the dual-stabilized platform, a_{E} and a_{N} are the eastward and northward horizontal accelerations of the carrier, and g_{m} is the gravity observations. The other is to determine the tilt angle of the platform before calculating the correction:

$$\delta a_{\mathrm{H}} = g_{\mathrm{m}}(\theta_x^2 + \theta_y^2)/2 - a_{\mathrm{E}x}\theta_x - a_{\mathrm{N}y}\theta_y, \tag{15}$$

where θ_x and θ_y are the horizontal and longitudinal tilt angles of the platform, and $a_{\mathrm{E}x}$ and $a_{\mathrm{N}y}$ are the horizontal and longitudinal components of a_{E} and a_{N} [59].

The above are commonly used correction models, in addition, some researchers have improved the model, such as M. Liu et al., who put forward a new correction model considering the influence of earth disturbance gravity and the horizontal component of Coriolis acceleration. The validity of the model was verified by the measured data [60].

The systematic errors of the atom gravimeter under static conditions, including light intensity noise, Raman wavefront distortion, and Zeeman frequency shift, will still have an impact on the measurement under dynamic conditions, but the magnitude is relatively small. So, it is not listed here; for details, see references [31,61,62] and so on.

4. Application Direction of Dynamic Measurement

MUQUANS [63] in France and AOSense in the United States have mature commercial products of compact, mobile, and high-precision atom gravimeters, but the research on dynamic measurement is still in its infancy, and there are no related mature products reported. Compared with static or stop-and-go measurements, gravity measurement during motion has unique application scenarios. Some possible application directions are listed below.

4.1. Gravity Field Mapping

High-precision gravity field mapping not only helps to accurately study the shape and internal structure of the earth but also reveals the law of the occurrence and development of spatial physical events near the earth, which is of great significance for resource exploration, geophysics, navigation, and environmental monitoring. Vehicle-borne, ship-borne, airborne, and space gravimeters are important gravity field mapping methods that can measure the gravity of forests, mountains, lakes, oceans, and other areas that are difficult for people to reach. Traditional gravity mapping is based on the relative gravimeter. The elastic fatigue of the spring causes the zero drift of the gravimeter. It needs to return to the reference point regularly or compare and calibrate with the absolute gravimeter, which seriously affects its mapping efficiency. The realization of dynamic measurement by an atom gravimeter makes the mapping of long-period gravity fields more efficient, continuous, and accurate. Some research teams have carried out related experiments. For example, ONERA, mentioned above, used the same set of atom gravimeters to carry out the ship-board and air-borne experiments. Gravity reference maps were drawn for both tests, and compared with the existing gravity field database, the accuracy was high, reaching the level of mGal or even sub-mGal [35,36]. It is expected that with the successful development

of more and more atom gravity dynamic measurement equipment and the emergence of commercial products, gravity field mapping will be its primary application field.

4.2. Navigation

An atom gravimeter is used in the field of navigation, which can collect high-precision gravity field information through real-time measurement, match it with the pre-measured gravity map database, and obtain the position information of the carrier, i.e., gravity-matching positioning. In addition, real-time and high-precision gravity field information can also directly improve mechanical arrangement and restrain inertial navigation error divergence, i.e., gravity compensation. The two are collectively referred to as gravity-assisted inertial navigation, which uses gravity information to improve the performance of inertial navigation from different aspects so as to realize the inertial navigation retuning under the condition of GNSS rejection, correct the error divergence with time, and improve the long-term stability.

The advantage of gravity-assisted inertial navigation lies in its strong concealment and the fact that there is no need to transmit or receive external signals, so it is a veritable passive navigation system. Compared with the commonly used relative gravimeter, the advantages of an atom gravimeter are high precision, no drift, and no need for regular return correction. These characteristics provide a guarantee for underwater navigation with high precision and long voyages. However, the realization of gravity-assisted inertial navigation requires not only high-precision gravity measurement equipment, which is currently available, but also high-precision, high-spatial-resolution gravity reference maps and reliable matching algorithms. At present, there is no global ocean gravity reference map with a hundred-meter-level spatial resolution that meets the requirements of underwater navigation [64], so gravity-assisted inertial navigation cannot be fully applied. It is expected that after the completion of large-area, high-precision gravity mapping in the future, the advantages of atom gravimeter dynamic measurement can be brought into full play in gravity-assisted inertial navigation.

Moreover, although most of the current atom interferometers are designed to be sensitive to acceleration in one direction, there is no fundamental limit to extending them to two- or three-dimensional measurement. Therefore, many researchers are committed to using quantum inertial sensors instead of traditional sensors to solve the problem of inertial navigation system error divergence with time and realize drift-free inertial navigation systems. In 2006, B. Canuel et al. developed an inertial navigation system measured entirely by atom interferometers. The atom cloud is emitted in a parabolic trajectory and interacts with the top Raman light, with four configurations providing measurements of angular velocity and acceleration in three directions. The angular velocity resolution was 1.4×10^{-7} rad/s (600 s), and the acceleration resolution was 64 uGal (600 s) [2]. In 2014, Akash V. Rakholia et al. demonstrated a dual-axis accelerometer and gyroscope, using two magneto-optical traps a few centimeters apart to trap atoms alternately, achieving a high data rate of 50 to 100 measurements per second with a sensitivity of 0.9 mGal/$\mathrm{Hz}^{1/2}$ and 1.1 (urad/s)/$\mathrm{Hz}^{1/2}$ [65]. The laboratory iXAtom, which is a collaboration between France's iXBlue and LP2N, aims to build an autonomous inertial device that does not rely on external correction. In 2016, the lab demonstrated a compact multi-axis atom interference accelerometer with a sensitivity of 230 mGal/$\mathrm{Hz}^{1/2}$ in the normal gravity and microgravity environments of parabolic aircraft [66,67]. In 2019, the team's B. Barrett et al. proposed a method to manipulate atom wavepackets in multiple spatial dimensions. Two-dimensional interference can separate the acceleration components in two directions and the angular velocity component in one excitation, and the two-dimensional interference superposition of three orthogonal planes can measure the acceleration and angular velocity of three axes. The system can also suppress laser phase noise and common system errors [68].

The use of quantum inertial devices to realize the drift-free inertial navigation system not only requires the device to have high precision but also needs to further increase its sampling bandwidth, which is the weak link of atom interference devices due to the

existence of dead time [44]. Therefore, there is still a long way to go before we realize the true benefits of high-precision and drift-free inertial navigation. At present, further research can be carried out on aspects of device configuration and combination with traditional devices.

4.3. Target Detection

Because the gravity information of large targets, such as submarines, cannot be concealed and camouflaged, target detection based on gravity has the advantage of anti-jamming. The magnitude of the gravity change caused by the target entering the detection area is related to its own mass. According to our calculation, taking the Ohio class submarine with a displacement of 18,700 tons as an example, when the distance above or below the detector is about 200 m, the regional gravity change is about μGal level [69], so the gravity measuring equipment is required to have high sensitivity. In addition, in order to cruise and detect in a large area, it is also required that the instrument can perform dynamic measurements. The atom gravimeter meets the above requirements and has great performance potential, so target detection is one of its possible application directions. But so far, the dynamic measurement accuracy and sensitivity of the atom gravimeter have not met the requirements. Mobile measurement can be considered for the time being, i.e., after the detector arrives in a certain area, target detection will be carried out after static deployment. Cruise detection will be implemented after a further breakthrough in the dynamic measurement performance of the atom gravimeter.

5. Conclusions

In this paper, the development history, principle, device, error source and suppression, and possible application direction of the atom gravimeter are introduced. The measurement accuracy of atom gravimeters under static or quasi-dynamic conditions has reached or even exceeded that of optical interference gravimeters. However, there are few reports on its dynamic measurement, and it is in the experimental stage. The atom gravimeter dynamic measurement maintains the stability of the measurement direction by adding a stabilized platform, which combines with the traditional accelerometer to solve the multi-value problem and restrain the vibration noise. Vibration noise, accelerometer error, and carrier dynamic effect are the main error sources of dynamic measurement, and their suppression and weakening are the keys to ensuring the measurement accuracy of an atom gravimeter. The application direction of an atom gravimeter for dynamic measurement is still in the exploratory stage. Compared with static measurement, an atom gravimeter may have unique advantages in the fields of gravity field mapping, navigation, and target detection.

Author Contributions: Conceptualization, A.L. and C.H.; Writing—original draft preparation, C.H.; writing—review and editing, F.Q.; funding acquisition, A.L. and F.Q. All authors have read and agreed to the published version of the manuscript.

Funding: This research was funded by the National Natural Science Foundation of China, grant number 42274013.

Institutional Review Board Statement: Not applicable.

Informed Consent Statement: Not applicable.

Data Availability Statement: Not applicable.

Conflicts of Interest: The authors declare no conflict of interest. The funders had no role in the design of the study; in the collection, analyses, or interpretation of data; in the writing of the manuscript; or in the decision to publish the results.

References

1. Kasevich, M.; Chu, S. Atomic interferometry using stimulated Raman transitions. *Phys. Rev. Lett.* **1991**, *67*, 181–184. [CrossRef] [PubMed]
2. Canuel, B.; Leduc, F.; Holleville, D.; Gauguet, A.; Fils, J.; Virdis, A.; Clairon, A.; Dimarcq, N.; Borde Ch, J.; Landragin, A.; et al. Six-axis inertial sensor using cold-atom interferometry. *Phys. Rev. Lett.* **2006**, *97*, 010402. [CrossRef] [PubMed]
3. Gustavson, T.L.; Bouyer, P.; Kasevich, M.A. Precision Rotation Measurements with an Atom Interferometer Gyroscope. *Phys. Rev. Lett.* **1997**, *78*, 2046–2049. [CrossRef]
4. Lamporesi, G.; Bertoldi, A.; Cacciapuoti, L.; Prevedelli, M.; Tino, G.M. Determination of the Newtonian Gravitational Constant Using Atom Interferometry. *Phys. Rev. Lett.* **2008**, *100*, 050801. [CrossRef] [PubMed]
5. Cladé, P.; de Mirandes, E.; Cadoret, M.; Guellati-Khélifa, S.; Schwob, C.; Nez, F.; Julien, L.; Biraben, F. Determination of the Fine Structure Constant Based on Bloch Oscillations of Ultracold Atoms in a Vertical Optical Lattice. *Phys. Rev. Lett.* **2006**, *96*, 033001. [CrossRef]
6. Chaibi, W.; Geiger, R.; Canuel, B.; Bertoldi, A.; Landragin, A.; Bouyer, P. Low frequency gravitational wave detection with ground-based atom interferometer arrays. *Phys. Rev. D* **2016**, *93*, 021101. [CrossRef]
7. Dimopoulos, S.; Graham, P.W.; Hogan, J.M.; Kasevich, M.A. Testing General Relativity with Atom Interferometry. *Phys. Rev. Lett.* **2007**, *98*, 111102. [CrossRef] [PubMed]
8. Geiger, R. Future Gravitational Wave Detectors Based on Atom Interferometry. In *An Overview of Gravitational Waves*; World Scientific: Toh Tuck, Singapore, 2016; pp. 285–313. [CrossRef]
9. Zhang, J.Y.; Chen, L.L.; Cheng, Y.; Luo, Q.; Shu, Y.B.; Duan, X.C.; Zhou, M.K.; Hu, Z.K. Movable precision gravimeters based on cold atom interferometry. *Chin. Phys.* **2020**, *29*, 093702. [CrossRef]
10. Wu, S.Q.; Li, T.C. The Technical Development of Absolute Gravimeter: Laser Interferometry and Atom Interferomery. *Acta Opt. Sin.* **2021**, *41*, 44–59. [CrossRef]
11. Geiger, R.; Ménoret, V.; Stern, G.; Zahzam, N.; Cheinet, P.; Battelier, B.; Villing, A.; Moron, F.; Lours, M.; Bidel, Y.; et al. Detecting inertial effects with airborne matter-wave interferometry. *Nat. Commun.* **2011**, *2*, 474. [CrossRef]
12. Geiger, R.; Landragin, A.; Merlet, S.; Santos, F.P.D. High-accuracy inertial measurements with cold-atom sensors. *AVS Quant. Sci.* **2020**, *2*, 024702. [CrossRef]
13. Peters, A.; Chung, K.Y.; Chu, S. High-precision gravity measurements using atom interferometry. *Metrologia* **2001**, *38*, 25–61. [CrossRef]
14. Muller, H.; Chiow, S.W.; Herrmann, S.; Chu, S.; Chung, K.Y. Atom-interferometry tests of the isotropy of post-Newtonian gravity. *Phys. Rev. Lett.* **2008**, *100*, 031101. [CrossRef] [PubMed]
15. Zhou, M.K.; Hu, Z.K.; Duan, X.C.; Sun, B.L.; Zhao, J.B.; Luo, J. Experimental progress in gravity measurement with an atom interferometer. *Front. Phys. China* **2009**, *4*, 170. [CrossRef]
16. Hu, Z.K.; Sun, B.L.; Duan, X.C.; Zhou, M.K.; Chen, L.L.; Zhan, S.; Zhang, Q.Z.; Luo, J. Demonstration of an ultrahigh-sensitivity atom-interferometry absolute gravimeter. *Phys. Rev. A* **2013**, *88*, 043610. [CrossRef]
17. Bidel, Y.; Carraz, O.; Charrière, R.; Cadoret, M.; Zahzam, N.; Bresson, A. Compact cold atom gravimeter for field applications. *Appl. Phys. Lett.* **2013**, *102*, 144107. [CrossRef]
18. Gillot, P.; Francis, O.; Landragin, A.; Pereira Dos Santos, F.; Merlet, S. Stability comparison of two absolute gravimeters: Optical versus atomic interferometers. *Metrologia* **2014**, *51*, L15–L17. [CrossRef]
19. Fang, B.; Dutta, I.; Gillot, P.; Savoie, D.; Lautier, J.; Cheng, B.; Alzar, C.; Geiger, R.; Merlet, S.; Pereira dos Santos, F.; et al. Metrology with Atom Interferometry: Inertial Sensors from Laboratory to Field Applications. *J. Phys. Conf. Ser.* **2016**, *723*, 012049. [CrossRef]
20. Gillot, P.; Cheng, B.; Imanaliev, A.; Merlet, S.; Santos, F.P.D. The LNE-SYRTE cold atom gravimeter. In Proceedings of the 2016 European Frequency and Time Forum (EFTF), York, UK, 4–7 April 2016; pp. 1–3.
21. Freier, C.; Hauth, M.; Schkolnik, V.; Leykauf, B.; Schilling, M.; Wziontek, H.; Scherneck, H.-G.; Müller, J.; Peters, A. Mobile quantum gravity sensor with unprecedented stability. *J. Phys. Conf. Ser.* **2015**, *723*, 012050. [CrossRef]
22. Wu, X.; Pagel, Z.; Malek, B.S.; Nguyen, T.H.; Zi, F.; Scheirer, D.S.; Müller, H. Gravity surveys using a mobile atom interferometer. *Sci. Adv.* **2019**, *5*, eaax0800. [CrossRef]
23. Huang, P.W.; Tang, B.; Chen, X.; Zhong, J.Q.; Xiong, Z.Y.; Zhou, L.; Wang, J.; Zhan, M.S. Accuracy and stability evaluation of the 85Rb atom gravimeter WAG-H5-1 at the 2017 International Comparison of Absolute Gravimeters. *Metrologia* **2019**, *56*, 045012. [CrossRef]
24. Zhang, X.; Zhong, J.; Tang, B.; Chen, X.; Zhu, L.; Huang, P.; Wang, J.; Zhan, M. Compact portable laser system for mobile cold atom gravimeters. *Appl. Opt.* **2018**, *57*, 6545–6551. [CrossRef]
25. Fu, Z.; Wang, Q.; Wang, Z.; Wu, B.; Cheng, B.; Lin, Q. Participation in the absolute gravity comparison with a compact cold atom gravimeter. *Chin. Opt. Lett.* **2019**, *17*, 011204. [CrossRef]
26. Wang, S.K.; Zhao, Y.; Zhuang, W.; Li, T.C.; Wu, S.Q.; Feng, J.Y.; Li, C.J. Shift evaluation of the atomic gravimeter NIM-AGRb-1 and its comparison with FG5X. *Metrologia* **2018**, *55*, 360–365. [CrossRef]
27. Bodart, Q.; Merlet, S.; Malossi, N.; Dos Santos, F.P.; Bouyer, P.; Landragin, A. A cold atom pyramidal gravimeter with a single laser beam. *App. Phys. Lett.* **2010**, *96*, 134101. [CrossRef]

28. Hinton, A.; Perea-Ortiz, M.; Winch, J.; Briggs, J.; Freer, S.; Moustoukas, D.; Powell-Gill, S.; Squire, C.; Lamb, A.; Rammeloo, C.; et al. A portable magneto-optical trap with prospects for atom interferometry in civil engineering. *Philos. Trans. R. Soc. A Math. Phys. Eng. Sci.* **2017**, *375*, 20160238. [CrossRef]
29. Wu, B.; Wang, Z.; Cheng, B.; Wang, Q.; Xu, A.; Lin, Q. The investigation of a μGal-level cold atom gravimeter for field applications. *Metrologia* **2014**, *51*, 452–458. [CrossRef]
30. Wang, Q.; Wang, Z.; Fu, Z.; Liu, W.; Lin, Q. A compact laser system for the cold atom gravimeter. *Opt. Commun.* **2016**, *358*, 82–87. [CrossRef]
31. Wu, B.; Zhou, Y.; Cheng, B.; Zhu, D.; Wang, K.-N.; Zhu, X.-X.; Chen, P.-J.; Weng, K.-X.; Yang, Q.-H.; Lin, J.-H.; et al. Static measurement of absolute gravity in truck based on atomic gravimeter. *Acta Phys. Sin.* **2020**, *69*, 25–32. [CrossRef]
32. Zhang, J.Y.; Xu, W.J.; Sun, S.D.; Shu, Y.B.; Luo, Q.; Cheng, Y.; Hu, Z.K.; Zhou, M.K. A car-based portable atom gravimeter and its application in field gravity survey. *AIP Adv.* **2021**, *11*, 115223. [CrossRef]
33. Mahadeswaraswamy, C. *Atom Interferometric Gravity Gradiometer: Disturbance Compensation and Mobile Gradiometry*; Stanford University: Stanford, CA, USA, 2009.
34. Cheng, B.; Chen, P.J.; Zhou, Y.; Wang, K.N.; Zhu, D.; Chu, L.; Weng, K.X.; Wang, H.L.; Peng, S.P.; Wang, X.R.; et al. The research on the experiment of dynamic absolute gravity measurement based on cold atom gravimeter. *Acta Phys. Sin.* **2022**, *71*, 247–257. [CrossRef]
35. Bidel, Y.; Zahzam, N.; Blanchard, C.; Bonnin, A.; Cadoret, M.; Bresson, A.; Rouxel, D.; Lequentrec-Lalancette, M.F. Absolute marine gravimetry with matter-wave interferometry. *Nat. Commun.* **2018**, *9*, 627. [CrossRef] [PubMed]
36. Bidel, Y.; Zahzam, N.; Bresson, A.; Blanchard, C.; Cadoret, M.; Olesen, A.V.; Forsberg, R. Absolute airborne gravimetry with a cold atom sensor. *J. Geod.* **2020**, *94*, 20. [CrossRef]
37. Bidel, Y.; Zahzam, N.; Bresson, A.; Blanchard, C.; Bonnin, A.; Bernard, J.; Cadoret, M.; Jensen, T.E.; Forsberg, R.; Salaun, C.; et al. Airborne absolute gravimetry with a quantum sensor, comparison with classical technologies. *J. Geophys. Res. Solid Earth* **2023**, *128*, e2022JB025921. [CrossRef]
38. Zhu, D.; Xu, H.; Zhou, Y.; Wu, B.; Cheng, B.; Wang, K.N.; Chen, P.J.; Gao, S.T.; Weng, K.X.; Wang, H.L.; et al. Data processing of shipborne absolute gravity measurement based on the extended Kalman filter algorithm. *Acta Phys. Sin.* **2022**, *71*, 159–167. [CrossRef]
39. Che, H.; Li, A.; Fang, J.; Ge, G.-G.; Gao, W.; Zhang, Y.; Liu, C.; Xu, J.-N.; Chang, L.-B.; Huang, C.-F.; et al. Research on ship-mounted dynamic absolute gravity measurement based on cold atom gravimeter. *Acta Phys. Sin.* **2022**, *71*, 148–156. [CrossRef]
40. Huang, C.F.; Li, A.; Qin, F.J.; Fang, J.; Chen, X. An atomic gravimeter dynamic measurement method based on Kalman filter. *Meas. Sci. Technol.* **2023**, *34*, 015013. [CrossRef]
41. Fang, J. Study on Compact Atom Gravimeters. Ph.D. Thesis, Huazhong University of Science and Technology, Wuhan, China, 2019.
42. Cheiney, P.; Fouché, L.; Templier, S.; Napolitano, F.; Battelier, B.; Bouyer, P.; Barrett, B. Navigation-Compatible Hybrid Quantum Accelerometer Using a Kalman Filter. *Phys. Rev. Appl.* **2018**, *10*, 034030. [CrossRef]
43. Cheiney, P.; Barrett, B.; Templier, S.; Jolly, O.; Battelier, B.; Bouyer, P.; Porte, H.; Napolitano, F. Demonstration of a Robust Hybrid Classical/Quantum Accelerometer. In Proceedings of the 2019 IEEE International Symposium on Inertial Sensors and Systems (INERTIAL), Naples, FL, USA, 1–5 April 2019; pp. 1–4.
44. McGuinness, H.J.; Rakholia, A.V.; Biedermann, G.W. High data-rate atom interferometer for measuring acceleration. *Appl. Phys. Lett.* **2012**, *100*, 011106. [CrossRef]
45. Tennstedt, B.; Schön, S. Integration of atom interferometers and inertial measurement units to improve navigation performance. In Proceedings of the 28th Saint Petersburg International Conference on Integrated Navigation Systems (ICINS), Saint Petersburg, Russia, 31 May–2 June 2021.
46. Lautier, J.; Volodimer, L.; Hardin, T.; Merlet, S.; Lours, M.; Pereira Dos Santos, F.; Landragin, A. Hybridizing matter-wave and classical accelerometers. *Appl. Phys. Lett.* **2014**, *105*, 144102. [CrossRef]
47. Wang, X.; Kealy, A.; Gilliam, C.; Haine, S.; Close, J.; Moran, B.; Talbot, K.; Williams, S.; Hardman, K.; Freier, C.; et al. Enhancing Inertial Navigation Performance via Fusion of Classical and Quantum Accelerometers. *arXiv* **2021**, arXiv:2103.09378.
48. Merlet, S.; Le Gouet, J.; Bodart, Q.; Clairon, A.; Landragin, A.; Dos Santos, F.P.; Rouchon, P. Operating an atom interferometer beyond its linear range. *Metrologia* **2009**, *46*, 87–94. [CrossRef]
49. Jimenez-Martinez, R.; Kolodynski, J.; Troullinou, C.; Lucivero, V.G.; Kong, J.; Mitchell, M.W. Signal Tracking Beyond the Time Resolution of an Atomic Sensor by Kalman Filtering. *Phys. Rev. Lett.* **2018**, *120*, 040503. [CrossRef]
50. Wu, B.; Cheng, B.; Fu, Z.-J.; Zhu, D.; Zhou, Y.; Weng, K.-X.; Wang, X.-L.; Lin, Q. Measurement of absolute gravity based on cold atom gravimeter at large tilt angle. *Acta Phys. Sin.* **2018**, *67*, 71–81.
51. Le Gouët, J.; Mehlstäubler, T.E.; Kim, J.; Merlet, S.; Clairon, A.; Landragin, A.; Pereira Dos Santos, F. Limits to the sensitivity of a low noise compact atomic gravimeter. *Appl. Phys. B* **2008**, *92*, 133–144. [CrossRef]
52. Zhou, M.K.; Hu, Z.K.; Duan, X.C.; Sun, B.L.; Chen, L.L.; Zhang, Q.Z.; Luo, J. Performance of a cold-atom gravimeter with an active vibration isolator. *Phys. Rev. A* **2012**, *86*, 043630. [CrossRef]
53. Tang, B.; Zhou, L.; Xiong, Z.; Wang, J.; Zhan, M. A programmable broadband low frequency active vibration isolation system for atom interferometry. *Rev. Sci. Instrum.* **2014**, *85*, 093109. [CrossRef] [PubMed]
54. Luo, D.Y.; Cheng, B.; Zhou, Y.; Wu, B.; Wang, X.; Lin, Q. Ultra-low frequency active vibration control for cold atom gravimeter based on sliding-mode robust algorithm. *Acta Phys. Sin.* **2018**, *67*, 82–87.

55. Richardson, L.L. Inertial Noise Post-Correction in Atom Interferometers Measuring the Local Gravitational Acceleration. Ph.D. Thesis, Leibniz University Hannover, Hannover, Germany, 2019.
56. Titan. Available online: https://nanometrics.ca/products/accelerometers/titan (accessed on 20 June 2022).
57. Yao, J.-M.; Zhuang, W.; Feng, J.-Y.; Wang, Q.-Y.; Zhao, Y.; Wang, S.-K.; Wu, S.-Q.; Li, T.-C. A coefficient searching based vibration correction method. *Acta Phys. Sin.* **2022**, *71*, 407–423. [CrossRef]
58. Gong, W.; Li, A.; Luo, J.; Che, H.; Ma, J.; Qin, F. A Vibration Compensation Approach for Atom Gravimeter Based on Improved Sparrow Search Algorithm. *IEEE Sens. J.* **2023**, *23*, 5911–5919. [CrossRef]
59. Huang, M.T.; Ning, J.S.; Ouyang, Y.Z.; Liu, M.; Lu, X.P.; Zhai, G.J.; Deng, K.L. Test and equivalent verification of gravity correction models for platform tilt in sea-borne and air-borne gravimeter. *Geom. Infor. Sci. Wuhan Uni.* **2016**, *41*, 738–744. [CrossRef]
60. Liu, M.; Huang, M.T.; Ma, Y.Y.; Ouyang, Y.Z.; Deng, K.L.; Lu, X.P.; Zhai, G.J. A modified correction model for platform tilt in air-sea-borne gravimetry. *Geom. Infor. Sci. Wuhan Uni.* **2018**, *43*, 586–591. [CrossRef]
61. Fu, Z.; Wu, B.; Cheng, B.; Zhou, Y.; Weng, K.; Zhu, D.; Wang, Z.; Lin, Q. A new type of compact gravimeter for long-term absolute gravity monitoring. *Metrologia* **2019**, *56*, 025001. [CrossRef]
62. Wu, B.; Zhu, D.; Cheng, B.; Wu, L.; Wang, K.; Wang, Z.; Shu, Q.; Li, R.; Wang, H.; Wang, X.; et al. Dependence of the sensitivity on the orientation for a free-fall atom gravimeter. *Opt. Exp.* **2019**, *27*, 11252–11263. [CrossRef] [PubMed]
63. Menoret, V.; Vermeulen, P.; Le Moigne, N.; Bonvalot, S.; Bouyer, P.; Landragin, A.; Desruelle, B. Gravity measurements below 10(-9) g with a transportable absolute quantum gravimeter. *Sci. Rep.* **2018**, *8*, 12300. [CrossRef] [PubMed]
64. Zheng, W.; Li, Z.L.; Wu, F. Research progress of the underwater gravity-aided navigation based on the information of aerospace-marine integration. *J. Natl. Uni. Def. Techno.* **2020**, *42*, 39–49. [CrossRef]
65. Rakholia, A.V.; McGuinness, H.J.; Biedermann, G.W. Dual-Axis High-Data-Rate Atom Interferometer via Cold Ensemble Exchange. *Phys. Rev. Appl.* **2014**, *2*, 054012. [CrossRef]
66. Barrett, B.; Antoni-Micollier, L.; Chichet, L.; Battelier, B.; Leveque, T.; Landragin, A.; Bouyer, P. Dual matter-wave inertial sensors in weightlessness. *Nat. Commun.* **2016**, *7*, 13786. [CrossRef]
67. Barrett, B.; Bertoldi, A.; Bouyer, P. Inertial quantum sensors using light and matter. *Phys. Scr.* **2016**, *91*, 053006. [CrossRef]
68. Barrett, B.; Cheiney, P.; Battelier, B.; Napolitano, F.; Bouyer, P. Multidimensional Atom Optics and Interferometry. *Phys. Rev. Lett.* **2019**, *122*, 043604. [CrossRef]
69. Qin, F.J.; Huang, C.F.; Li, D.Y.; Chang, L.B.; Li, K.L.; Zhu, J.P.; Che, H.; Di, J.B.; Gao, D.Y.; Jiang, S. Underwater Target Detection Method and System Based on Gravity Information. Patent CN112859186B, 15 April 2022.